

Nitrogen doped graphene supported Pt-Pd nanoparticle modified GC electrode for electrochemical determination of tramadol and paracetamol

Janakiraman Manokaran, Jonna Narendranath,
Rethinasabapathy Muruganatham & Natesan Balasubramanian*

Department of Chemical Engineering, AC Tech Campus, Anna
University, Chennai 600 025, India

Email: nbsbala@annauniv.edu; nbsbala@gmail.com

Received 15 March 2016; revised and accepted 26 December 2016

The role of functionalized nitrogen doped graphene (NGp) using poly(diallyldimethylammonium chloride) (PDDA) as modified electrode has been discussed. Pt-Pd bimetallic nanoparticles have been anchored on PDDA-NGp to form PtPd-PDDA-NGp nanocomposites, which are characterized by high resolution transmission electron microscope, X-ray diffraction and Raman spectroscopy. The simultaneous determination of paracetamol and tramadol has been carried out using the nitrogen doped graphene supported Pt-Pd nanoparticle modified glassy carbon electrode in 0.1 M Britton-Robinson buffer solution (pH 5.0). Two well-defined voltammetric peaks are obtained in square wave voltammogram measurements. It has been observed that the modified electrode can detect a wide linear range of concentrations of paracetamol from 5×10^{-6} to 1×10^{-4} M, and tramadol from 1.2×10^{-5} to 2.4×10^{-4} M. The limit of detection was found to be 1.8×10^{-7} and 5.7×10^{-6} M for paracetamol and tramadol, respectively ($S/N = 3$).

Keywords: Electrochemistry, Electroanalysis, Graphene, Doped graphene, Electrodes, Modified electrodes, Paracetamol, Tramadol

Tramadol (TD) and paracetamol (PA) are electroactive molecules, which act as analgesic and antipyretic drugs¹. TD possesses μ -opioid properties and activates monoaminergic spinal inhibition of pain, and is also effective in relieving postoperative pain, moderate surgical pain, surgical pain in children and cancer pain. An overdose of TD has a risk of death and life-threatening side effects, such as slowed or stopped breathing, dangerous changes in heart beats and even death²⁻⁶. PA is an effective pain killer for backache, headache, arthritis and postoperative pain, and is also used for the treatment of fevers of bacterial or viral origin⁷⁻⁹. PA is metabolized predominantly in the liver, where it generates toxic

metabolites. Overdose ingestions of PA lead to the accumulation of toxic metabolites, which may cause severe and sometimes fatal hepatotoxicity and nephrotoxicity, in some cases, is associated with renal failure^{10, 11}. Therefore, the development of a simple, inexpensive and precise analytical method for the determination of TD and PA in therapeutic samples is of at most importance.

The determination of TD and PA can be carried out by using several methods such as GC-MS^{12,13}, LC-MS^{14,15}, HPLC^{16,17}, second derivative spectroscopy¹⁸, fluorimetry¹⁹, chemiluminescence, ion-exchange column chromatography, spectrophotometry, pseudopolarography and capillary electrophoresis⁷. However, these techniques suffer from some disadvantages like time consumption, high cost, and tedious sample pretreatment procedures. Therefore, it is necessary to develop new analytical methods having high sensitivity, low detection limit, low cost and high precision for the determination of TD and PA.

Electrochemical approaches have shown significant benefits in the analysis of biomolecules in therapeutic treatment and human body fluids. Several electrochemical techniques exist for the determination of TD and PA. However, voltammetric method is suitable for the simultaneous determination of TD and PA²⁰. In the electrochemical determination, the unmodified electrodes like carbon paste electrode (CPE), glassy carbon electrode (GCE), PVC membrane electrode, gold and platinum electrodes used for the analyses have some limitations, such as low electron transfer rate and overlapping of voltammetric peaks²¹⁻²⁴.

More recently, metallic nanoparticles composed of CNTs or graphene-modified electrodes have been reported to show low ohmic resistance, fast electron transfer rate, low overpotential, low background current and negligible surface fouling^{25,26}. Of particular interest are nanocomposites involving gold nanoparticles (AuNPs) with CNTs or graphene, which exhibit unique electronic properties along with the biocompatibility and electrocatalytic effects^{27,28}. Some modified electrodes which have the above properties, i. e., AuNPs/CNTs⁵, MWCNT/CPE⁶, AuNP/MWNT/ITO⁹, D50wx2/GNP/GCPE²⁰ and Au-nanochains/MWCNTs/GC²⁹, have been reported.

N-doped graphene exhibits enhanced metallic behavior and excellent biocompatibility^{30, 31}. In the present study, we have aimed at stacking Pt-Pd NPs on N-doped graphene, which will have greater active surface areas, upgraded charge transfer kinetics and excellent electrocatalytic properties due to the bimetallic synergistic effect. PtPdNps-NGp composite acts as 'electron wire' to transfer the electron between the electroactive (TD/PA) molecules and electrode surface. These nanocomposites materials can be used as a modified electrode for the assembling of an electrochemical sensor.

Experimental

Graphite flakes, H₂SO₄, KMnO₄, hydrogen peroxide, hydrazine monohydrate, polydiallyldimethylammonium chloride (PDDA, 20 wt%, in H₂O), hexachloroplatinum(IV) acid hydrate (H₂PtCl₆.6H₂O) and palladium(II) chloride (PdCl₂) were purchased from Sigma-Aldrich. A Britton-Robinson (BR) buffer solution was prepared using boric acid, acetic acid and sodium hydroxide pellets. Sodium borohydride, tramadol hydrochloride injection (supridol), paracetamol tablets, and infected human urine samples (containing paracetamol and tramadol) were collected from The Health Center, Anna University, Chennai, India.

The morphologies of the prepared samples were observed with HRTEM images recorded on a Tecnai-G2 (model T-30) S-twin instrument at an accelerating voltage of 300 kV. X-ray diffraction (XRD) patterns were recorded on a Bruker D8 diffractometer with Cu K α radiation ($\lambda = 1.5418 \text{ \AA}$). The Raman shifts of these samples were analyzed, by using a Jobin-YvonLabRam HR spectrometer with an exciting source (514 nm Ar laser).

All the electrochemical studies were executed in a three-electrode cell, using a CHI660D electrochemical workstation. A glassy carbon (GC) electrode of geometric area (0.07 cm²) was used as a working electrode, while a Pt wire with high geometrical surface area (20 cm²) and a saturated calomel electrode (SCE) were used as counter electrode and reference electrode, respectively. All the electrochemical measurements were made in an inert atmosphere, by purging N₂ gas for 30 min into the BR buffer solutions, which acted as the supporting electrolyte.

The GC electrode was physically cleaned with mirror polish cloth using fine grade alumina powders

of decreasing particle size (1, 0.3 and 0.5 μm), then washed with Millipore water and cleaning solution. The electrochemical cleaning of GC electrode was done by cyclic voltammetric method in 0.1 M H₂SO₄ (scanning between -0.2 V and 1.2 V for 50 cycles). The sample, PtPd-PDDA-NGp (2 mg) was dispersed in ethanol (1 mL) and sonicated for 10 min. Finally, the dispersion was uniformly coated over the surface of GCE using the drop coat method and dried.

For the synthesis of nitrogen doped graphene supported Pt-Pd (PtPd-PDDA-NGp) nanocomposite, conc. sulphuric acid (60 mL) was mixed with 100 mg of graphite flakes in a 250 mL RB flask, then the mixture was sonicated for 2 h, and 500 mg of potassium permanganate was gradually added to the RB flask. During the process, the temperature was maintained at 5 °C. Then the mixture was stirred for 24 h at 35 °C. After 24 h, 300 mL water (Millipore) was added to the mixture at 5 °C followed by constant stirring at room temperature for 2 h. Finally, the reaction mixture was centrifuged and the product was washed several times with Millipore water and dried. GO (80 mg) was mixed with hydrazine monohydrate (27 μL) and the reaction mixture was stirred at 80 °C for 1 day. After cooling to room temperature, nitrogen-doped graphene (NG) was obtained by filtering and drying³². PDDA (2 mL of 20% solution) was added dropwise into 60 mg of nitrogen-doped graphene (NG) under vigorous stirring for 24 h. Then the mixture was centrifuged to remove the unreacted PDDA.

In a typical method for the preparation of Pt-Pd nanoparticles, 40 mg of PDDA-NG in aqueous medium was purged with nitrogen gas for 1 h under constant stirring. Then equimolar amounts (10 mM) of Pt and Pd solution were added dropwise into the reaction mixture. Sodium borohydride (0.1 M) was added dropwise into the reaction mixture to form the PtPd-PDDA-NGp nanocomposite.

Results and discussion

The HRTEM images of the nitrogen doped graphene and the sample after coating with PDDA show that the positive charged PDDA is effectively coated on electronegative nitrogen doped graphene surface (Fig. 1(a&b)). The deposition of Pd-Pt nanoparticles over the surface of the positive charged PDDA coated NGp nanocomposite is shown in Fig. 1(c). NGp shows a broad peak at 25.3° corresponding to the (002) plane (Fig. 2a), which

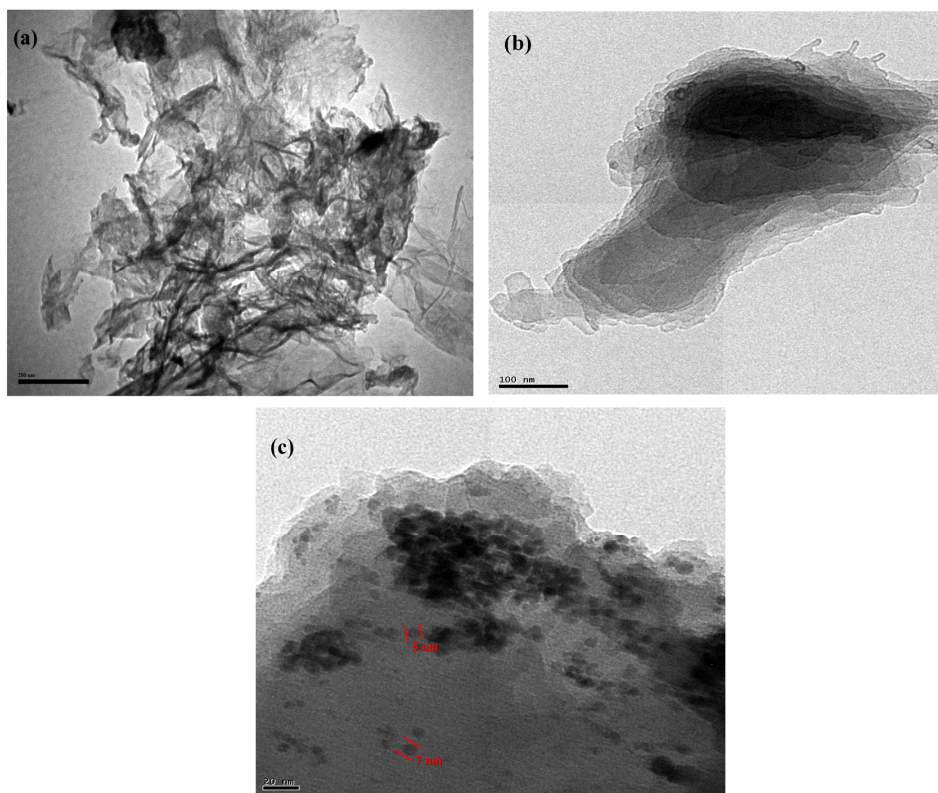


Fig. 1 – HRTEM images of (a) NGp (b) PDDA-NGp, and, (c) PtPd-PDDA-NGp.

indicates that the nitrogen is hosted on the graphene lattice to form a restacked crystalline structure³³⁻³⁵. On compositing PDDA with NGp, there was a broadening of peak with a decrease in intensity (Fig. 2b). This confirms the adherence of PDDA over the surface of NGp. The Pt-Pd nanoparticle loaded PDDA-NGp shows three characteristic peaks at 39.5°, 46.2°, and 67.6°, which corresponds to (111), (200), and (220) planes of Pd and Pt respectively (JCPDF 65-6418) (Fig. 2c)^{36,37}. The (002) plane of NGp is shifted slightly to lower theta value and the peak is broad due to formation of smaller sized nanoparticles.

The Raman spectra of NGp shows two prominent bands at 1346 and 1576 cm^{-1} , which are denoted as the D and G bands, respectively (Fig. S1, Supplementary data). The D band is due to defects in the curved graphene sheet (k point phonons of A_{1g} symmetry), whereas the G band corresponds to sp^2 hybridized graphitic carbon (stretching mode of crystal graphite, the zone center of the E_{2g} mode). The I_D/I_G value of NGp was found to be 1.46 due to the intercalation of nitrogen atoms^{34, 38, 39}. The presence of N dopant on graphene was confirmed by the 2D overtone of the D band at around 2719 cm^{-1} and

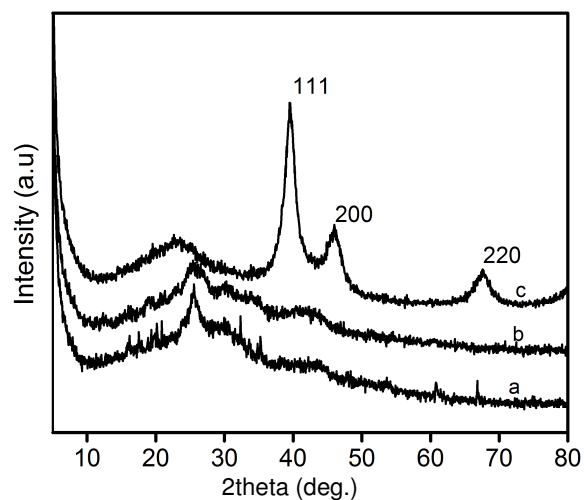


Fig. 2 – XRD patterns of (a) NGp, (b) NGp-PDDA, and, (c) NGp-PDDA/PtPd.

combination bands (D+G) around 2925 cm^{-1} (ref. 40). After PDDA functionalization, the I_D/I_G value of NGp decreases from 1.46 to 0.94. Further, the 2D and (D+G) bands are overlapped which results in peak broadening confirming the functionalization of PDDA

over NGp surface. The presence of Pt-Pd nanoparticles on PDDA functionalized NGp was confirmed by the increase in I_D/I_G value to 0.981 and the reoccurrence of (D+G) band

The effect of pH of the supporting electrolyte (0.1 M BR buffer solution) on the PtPd-PDDA-NGp modified GC electrode towards PA ($3.6 \times 10^{-5} M$) and TD ($4.8 \times 10^{-5} M$) was carried out by increasing the pH from 1 to 12. It was found that there was no significant current response of PA and TD oxidation in $pH < 3$ and $pH > 9$. It was observed that the oxidation peak potential (E_p) of PA and TD increases, with an increase in pH from 3 to 9. At pH 7.0, PA and TD oxidize at potentials of 0.31 V and 0.64 V with higher current responses of $5.26 \times 10^{-5} A$ and $2.02 \times 10^{-4} A$, respectively. This suggests that the optimum pH for the PtPd-PDDA-NGp modified GC electrode is 7 (ref. 41).

Figure 3 shows the cyclic voltammograms of PA ($3.6 \times 10^{-5} M$) and TD ($4.8 \times 10^{-5} M$) obtained, with the supporting electrolyte of pH 7, employing varying scan rates from 10 to 250 mV/s. The calibration plots of the PA and TD peak currents (I_p) increase linearly with an increasing scan rate (v), which confirms that the process takes place in the modified electrode is diffusion controlled.

$$I_{pa} (\mu A) = 1.5019 \times 10^{-7} (v) (mV s^{-1}) + 1.8429 \times 10^{-5} \quad (R^2 = 0.9956) \text{ for PA.}$$

$$I_{pa} (\mu A) = 5.3579 \times 10^{-7} (v) (mV s^{-1}) + 5.4316 \times 10^{-5} \quad (R^2 = 0.9959) \text{ for TD.}$$

The double logarithmic plots give the slope values of PA and TD as 0.5331 and 0.5679, respectively. The slope values less than 1 confirms that the reaction

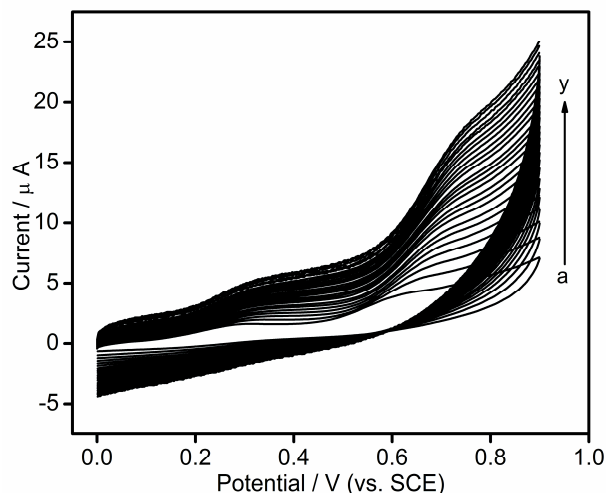


Fig. 3 – CVs of PtPd-PDDA-NGp/GCE in PA and TD ($pH = 7.0$) at different scan rates (a to y: 10 to 250 $mV s^{-1}$).

which takes place at the modified electrode is diffusion controlled.

$$\log I_{pa} (\mu A) = 0.5314 (\log v) (mV s^{-1}) - 0.5371 \quad (R^2 = 0.9956) \text{ for PA.}$$

$$\log I_{pa} (\mu A) = 0.5269 (\log v) (mV s^{-1}) - 0.0054 \quad (R^2 = 0.9959) \text{ for TD.}$$

Figure 4 shows the square wave voltammograms (SWV) of PA (1×10^{-5} to $2 \times 10^{-4} M$) by keeping the concentration of TD at a constant value of $3.60 \times 10^{-4} M$ at the PtPd-PDDA-NGp modified GCE. Two well pronounced peaks are observed around 0.184 and 0.580 V. The SWV peak current is in a linear relationship with increasing concentration of PA. The

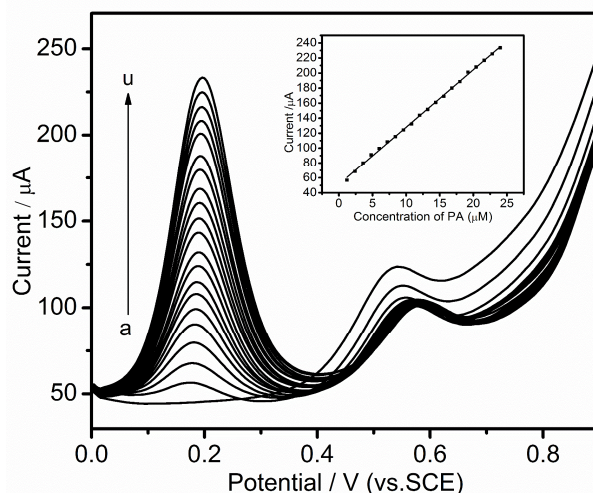


Fig. 4 – Square wave voltammograms for increasing concentration of PA ($1 \times 10^{-5} M$ to $2 \times 10^{-4} M$) in the presence of $3.60 \times 10^{-4} M$ TD at the PtPd-PDDA-NGp modified GCE.

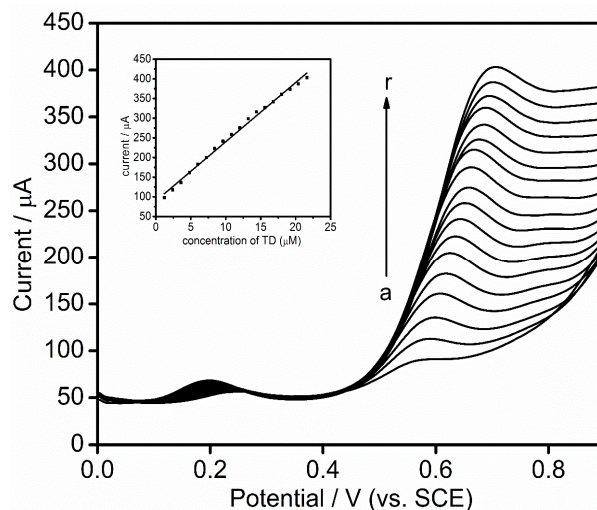


Fig. 5 – Square wave voltammograms for increasing concentration of TD ($1 \times 10^{-5} M$ to $2 \times 10^{-4} M$) in the presence of $2.40 \times 10^{-5} M$ PA at the PtPd-PDDA-NGp modified GCE.

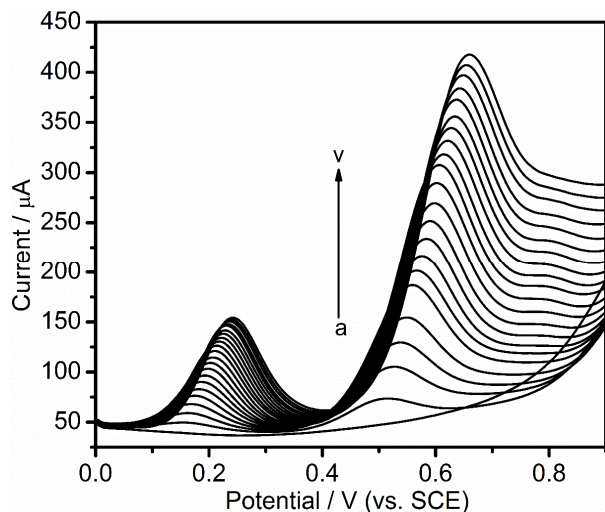


Fig. 6 – Square wave voltammograms obtained for simultaneous determination of PA (5×10^{-6} to 1×10^{-4} M) and TD (1.2×10^{-5} to 2.4×10^{-4} M) in pH 7 solution at PtPd-PDDA-NGp modified GCE.

limit of detection (LOD) value of PA is 4.4389×10^{-7} M, with the linear regression equation as: $I (\mu\text{A}) = 0.765C_{\text{PA}} (M) + 5.4694$, $R^2 = 0.9989$ for PA.

Square wave voltammograms for the concentration variation of TD from 1.2×10^{-5} M to 1.92×10^{-4} M and the linear concentration range of the PtPd-PDDA-NGp modified GC electrode in the presence of 2.40×10^{-5} M of PA is shown in Fig. 5. The limit of detection for TD is found to be 3.6526×10^{-6} M, while the linear regression equation is: $I (\mu\text{A}) = 1.5049C_{\text{TD}} (M) + 8.9673 \times 10^{-5}$, $R^2 = 0.9989$ for TD.

Simultaneous determination of PA and TD by varying the concentration of PA from 5×10^{-6} to 1×10^{-4} M, and that of TD from 1.2×10^{-5} to 2.4×10^{-4} M is shown in Fig. 6. Both the systems show two linear ranges of calibration curves. When the concentrations of PA and TD increase, the oxidation potential of these two systems shift to the positive potential range due to the ionic interaction at the surface of the modified electrode, thereby resulting in two linear ranges. The LOD values of PA and TD are found to be 1.8×10^{-7} , 5.7×10^{-6} M respectively.

We have studied the interference of several compounds such as dopamine, L-dopa, L-alanine, L-glutamic acid, uric acid, ascorbic acid, and aspartic acid. It has been observed that the oxidation peak current and potential of PA and TD were not altered due to the presence of 100-fold surplus of these interfering compounds.

The stability of PtPd-PDDA-NGp modified GCE was observed by recording the oxidation peak current

of PA (2.5×10^{-5} M) and TD (4.8×10^{-5} M) at pH 7 by square wave voltammetry. Over a period of 5 min intervals for 50 repetitive measurements, the modified electrode retained 98% of its initial oxidation peak current, which indicates the good stability of the modified electrode. The reproducibility of the modified electrode was measured at four electrodes separately prepared under the same concentration as mentioned above. The results reveal that the modified electrode has acceptable reproducibility, with an RSD of 5%.

The amounts of PA and TD present in the infected human urine sample were analyzed by the standard addition method using the PtPd-PDDA-NGp modified electrode. The amounts of PA and TD in the infected urine samples were detected with RSD of 1.2 and 0.9% respectively.

The present study indicates that NGp-PDDA supported Pt-Pd nanoparticle modified electrode exhibits excellent electrocatalytic activity towards the oxidation of PA and TD. In addition, it has been shown that this composite has high stability, selectivity, sensitivity and reproducibility. The modified electrode detects PA over a wide linear range of concentration from 5×10^{-6} to 1×10^{-4} M, and TD from 1.2×10^{-5} to 2.4×10^{-4} M. The limit of detection was found to be 1.8×10^{-7} and 5.7×10^{-6} M for PA and TD, respectively ($S/N = 3$).

Supplementary data

Supplementary data associated with this article, i.e., Fig. S1, is available in the electronic form at [http://www.niscair.res.in/jinfo/ijca/IJCA_56A\(01\)63-68_SupplData.pdf](http://www.niscair.res.in/jinfo/ijca/IJCA_56A(01)63-68_SupplData.pdf).

Acknowledgement

This work has been supported by Anna University, Chennai, India, under the Anna Centenary Research Fellowship (ACRF) scheme vide Lr. No.CR/ACRF/2013/27.

References

- Habibi B, Jahanbakhshi M & Azar M H P, *Anal Biochem*, 411, (2011) 167.
- Afrasiabi M, Zad Z R, Kianipour S, Babaei A & Taheri A R, *J Chem Soc Pak*, 35 (2010) 1106.
- Houmes R J M, Voets M A, Verkaaik A, Erdmann W & Lachmann B, *Anesthesia Analgesia*, 74 (1992) 510.
- Afkhami A, Ghaedi H, Madrakian T, Ahmadi M & Kashani H M, *Biosensors Bioelectr*, 44 (2013) 34.
- Atta N F, Ahmed R A, Amin H M A & Galal A, *Electroanalysis*, 24 (2012) 2135.
- Soleimani M, Afshar M G, Shafaat A & Crespo G A, *Electroanalysis*, 25 (2013) 1159.

- 7 Atta N F, Kady M F & Galal A, *Sensors Actuators B*, 141(2009) 566.
- 8 Boopathi M, Won M S & Shim Y B, *Anal Chim Acta*, 512 (2004) 191.
- 9 Goyal R N, Rana A R, Aziz M A & Oyama M, *Anal Chim Acta*, 35 (2011) 35.
- 10 Habibia B, Jahanbakhshia M & PAzarb M H, *Electrochim Acta*, 56 (2011) 2888.
- 11 Maria S M Q, Araki K, Toma H E & Angnes L, *Electroanalysis*, 14 (2002) 1629.
- 12 Chytil L, Sticha M, Matouskova O, Perlik F & Slanar O, *J Chromatogr B*, 877 (2009) 1937.
- 13 Cheng P S, Lee C H, Liu C & Chien C S, *J Anal Toxicol*, 32 (2008) 253.
- 14 Musshoff F, Madea B, Stuber F, & Stamer U M, *J Anal Toxicol*, 30 (2006) 463.
- 15 Zhu T, Ding L, Guo X, Yang L & Wen A, *Chromatographia*, 66 (2007) 171.
- 16 Belal T, Awad T & Clark C R, *Chromatogr Sci*, 47 (2009) 849.
- 17 Ardakani Y H, Foroumadi R A & Rouini M R, *J Chromatogr B*, 864 (2008) 109.
- 18 Toral M I, Rivas J, Saldías M, Soto C & Orellana S, *J Chil Chem Soc*, 53 (2008) 1543.
- 19 Nohta H, Yukizawa T, Ohkura Y, Yoshimura M, Ishida J & Yamaguguchi M, *Anal Chim Acta*, 344 (1997) 233.
- 20 Sanghavi B J & Srivastava A K, *Anal Chim Acta*, 706 (2011) 246.
- 21 Abu-Shawish H M, Ghalwa N A, Zaggout F R, Saadeh S M, Al-Dalou A R & Assi A A, *Biochem Eng J*, 48 (2010) 237.
- 22 Atta N F, El-Kady M F & Galal A, *Sensors Actuators B*, 141 (2009) 566.
- 23 Chen J & Cha CS, *J Electroanal Chem*, 463 (1999) 93.
- 24 Dayton M A, Ewing A G & Wightman R M, *Anal Chem*, 52 (1980) 2392.
- 25 Guo S & Dong S, *Trends Anal Chem*, 28 (2009) 96.
- 26 Guo S, Li J, Ren W, Wen D, Dong S & Wang E, *Chem Mater*, 21 (2009) 2247.
- 27 Valentini F, Amine A, Orlanducci S, Terranova M L & Palleschi G, *Anal Chem*, 75 (2003) 5413.
- 28 Mahmoud K A, Hrapovic S & Luong J HT, *ACS Nano*, 2 (2008) 1051.
- 29 Manoj D, Kumar DR & Santhanalakshmi J, *Anal Methods*, 5 (2013) 3503.
- 30 Sheng ZH, Zheng X, Xu J, Bao W, Wang F & Xia X, *Biosensors Bioelectronics*, 34 (2012) 125.
- 31 Wang Y, Shao Y, Matson D W, Li J, & Lin Y, *ACS Nano*, 4 (2010) 1790.
- 32 Park S, Hu Y, Hwang J, Lee E, Casabianca L B, Cai W, Potts J R, Ha HW, Chen S, Ishii Y & Ruoff R S, *Nature Commun*, 3 (2012) 1.
- 33 Tsai C W, Tu M H, Chen C J, Hung T F, Liu R S, Liu W R, Lo M Y, Peng Y M, Zhang L, Zhang J, Shy DS & Xing X K, *RSC Adv*, 1 (2011) 1349.
- 34 Dai Z, Wang K, Li L & Zhang T, *Int J Electrochem Sci*, 8 (2013) 9384.
- 35 Mowrya M, Palaniuka D, Luhrs C C & Osswald S, *RSC Adv*, 3 (2013) 21763.
- 36 Yang X, Yang Q, Xua J & Lee C S, *J Mater Chem*, 22 (2012) 8057.
- 37 Zhang H, Xu X, Gu P, Li C, Wu P & Cai C, *Electrochim Acta*, 56 (2011) 7064.
- 38 Chen S, Duan J, Ran J, Jaronecb M & Qiao S Z, *Energy Environ Sci*, 6 (2013) 3693.
- 39 Wang H, Maiyalagan T & Wang X, *ACS Catal*, 2 (2012) 781.
- 40 Huang H & Wang X, *J Mater Chem*, 22 (2012) 22533.
- 41 Bidkorbeh F G, Shahrokhiana S, Mohammadi A, Dinarvand R, *Electrochim Acta*, 55 (2010) 2752.